The Retroflection of the Agulhas Current

J. R. E. LUTJEHARMS AND R. C. VAN BALLEGOOYEN

National Research Institute for Oceanology, CSIR, Stellenbosch, South Africa

(Manuscript received 29 December 1987, in final form 25 April 1988)

ABSTRACT

A description of the nature and kinematics of the Agulhas Current termination is given based on satellite infrared imagery and selected hydrographic measurements collected over the past decade. On average the Agulhas retroflection lies between 16° and 20°E longitude and has a loop diameter of 340 km. During the period of the investigation the retroflection loop protruded into the South Atlantic at intervals of slightly more than one month, shedding a pinched-off Agulhas ring with a diameter of about 320 km at its most westerly extension. Rings drift away at about 12 cm s^{-1} and can be observed by their distinctive thermal characteristics at the sea surface as far west as 5°E and as far south as 46°S, well south of the subtropical convergence. The shedding rate of rings and their subsequent drift may play an important role in the dynamics of the South Atlantic Ocean.

1. Introduction

As a major western boundary current the Agulhas Current exhibits a unique and consistent downstream circulation feature that consists of a prominent turnabout at which the current direction is more or less reversed, the Agulhas retroflection. We report here the results of an investigation spanning about seven years during which the kinematics and behavior of the retroflection of the Agulhas Current have been studied.

Unlike the northern reaches of the Agulhas Current (Pearce 1977), the southern reaches have not been investigated intensively until lately. Results of a major three-ship cruise initiated by Bang (1970) showed for the first time the inherent generic nature of the Agulhas retroflection and that the terminal region of the Agulhas Current was populated by a range of eddies. Deep-sea eddies had been observed in the region prior to this time (Duncan 1968), but these latter quasi-synoptic data intimated the connection between the Agulhas Current and these features (Harris and van Foreest 1978). Furthermore, a study using serial satellite imagery showed that the Agulhas retroflection was unstable, and that it could coalesce and form Agulhas rings (Lutjeharms 1981b) with an average diameter of 320 km (Lutjeharms 1981a).

The factor responsible for the singular current behavior manifested in the retroflection may stem from the principle of conservation of potential vorticity. To test this the current may be modeled as a free inertial jet (Gill and Schumann 1979) and Lutjeharms and van Ballegooyen (1984) have successfully modeled the retroflection in this manner under a range of possible conditions. A net poleward flow in the model can be sustained if the planetary vorticity change on moving poleward is balanced by increasing depth of the current. Because the depth is limiting, the current has to change direction. The model shows that the volume transport of the current is a decisive factor which regulates the position of retroflection.

De Ruijter (1982), on the other hand, has modeled the current from the point of a large-scale wind-driven ocean circulation incorporating inertia; he has shown that the existence of a retroflection is critically dependent on the wind stress curl decreasing substantially in a region adjacent to South Africa which can still be considered to form part of an inertial boundary layer. Subsequently, de Ruijter and Boudra (1985) have also found that the Agulhas retroflection is largely due to the net accumulation of anticyclonic relative vorticity as the current flows southward. Including baroclinicity in their model (Boudra and de Ruijter 1986) has facilitated the simulation of ring formation at the retroflection.

Recent shipboard investigations (Gordon et al. 1987) have underscored the key role this area plays in the ventilation of the Atlantic and Indian Ocean thermocline through an exchange of water south of Africa (Gordon 1985). This process has been shown to depend to a large extent on ring shedding at the Agulhas retroflection (Lutjeharms and Gordon 1986; Olson and Evans 1986). The frequency of this shedding and the mean location of the retroflection, as well as its general behavior, is presently unknown, but it is clearly significant in gaining a better understanding of the inter-

Corresponding author address: Dr. J. R. E. Lutjeharms, Division of Earth, Marine and Atmospheric Science and Technology, CSIR, P.O. Box 320, Stellenbosch 7600, South Africa.

ocean exchange processes taking place south of Africa as well as in suggesting the key relevant mechanisms. Using a number of available data sources covering an extensive period, we present some general descriptive results on the kinematics of the Agulhas retroflection and its direct oceanic environment.

2. Data and methods

The data used in this investigation consist of a collection of thermal infrared images and a number of thermal ocean sections obtained from expendable bathythermograph measurements, all spanning nearly ten years.

Thermal infrared data measured in the range between 10.5 and 12.5 μm over this ocean area are from the radiometers on board the geostationary satellites METEOSAT I and II, the Very High Resolution Radiometers (VHRR) on board the near-polar orbiting satellites NOAA 4 and 5 and the Advanced Very High Resolution Radiometers (AVHRR), measuring in the

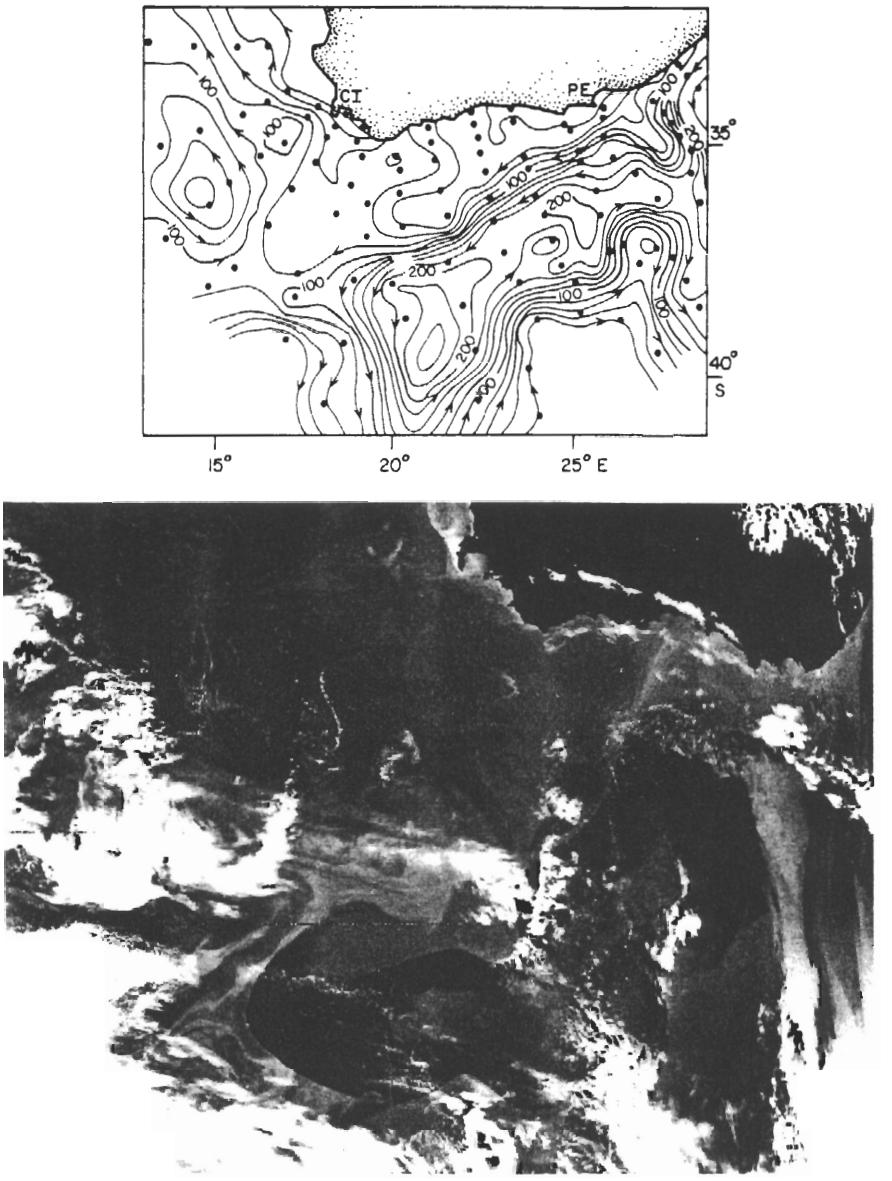

FIG. 1. The Agulhas retroflection as manifested in, (a) hydrographic data, and (b) satellite remote sensing. Both frames show approximately the same geographical area, with the southern coast of Africa at the top and the locations of Cape Town (CT) and Port Elizabeth (PE) shown in (a). The satellite image is in the thermal infrared from the AVHRR of the NOAA 9 satellite for 13 November 1985. Dark hues indicate warmer water. The hydrographic measurements show the depth of the sigma-t 25.80 surface during the Combined Agulhas Cruise of March 1969.

range 10.5 to 11.5 μm, of the NOAA 6, 7, TIROS N and Nimbus 7 satellites. The nadir resolution at the equator for the geostationary satellites is 5 × 5 km, and between 800 and 1.4 km along the subsatellite track for the orbiting satellites. Persistent cloudiness over the geographic area of interest occurs between 70 and 80 percent of the time (Lutjeharms and Valentine 1988), which means that continuous serial measurements over lengthy periods are rarely possible and that the utility of satellite imagery south of 40°S is limited. METEOSAT II images for 1985 only have routinely been "declouded" (Boyle and Howe 1985) by combining a number of sequential images of each day to minimize cloud cover. This has increased the useful coverage of the area significantly for this particular period. Images used for this investigation were geometrically uncorrected so that geographic positioning is estimated to be correct only to 20 to 30 km. No atmospheric corrections were made to this particular dataset, but experience with such corrections has subsequently shown (J. J. Agenbag, personal communication 1987) that horizontal thermal gradients are so extreme in this ocean area that the geographic location of ocean fronts are not much affected by such corrections. Changes in surface thermal distributions, as indicated by satellite infrared imagery, may be interpreted as being due to lateral movements only. This may be erroneous if surface heating by insolation or upward vertical movement of colder water is a dominant mechanism in the area. With the present data these distinctions cannot be made, but experience from numerous measurements in the area have demonstrated the high vertical coherence in the temperature field (Harris and van Foreest 1978; Lutjeharms and Valentine 1984, 1987), establishing the representativeness of most surface readings for the upper water column as a whole.

Expendable bathythermograph (XBT) readings were undertaken from 1978 to 1986 from ships of opportunity. Numerous crossings of the Agulhas retroflection region afforded an opportunity to gather data here. Bathythermograph traces have been calibrated and have undergone a quality control. This methodology has been described in detail elsewhere (Lutjeharms and Emery 1983) and is not repeated here.

3. General description of the Agulhas retroflection

The Agulhas retroflection is very prominent in cloudpoor satellite images of the area. A characteristic example is given in Fig. 1b where the current extends westward to about 17°E. The narrow warm ribbon of the Agulhas Current, about 90 km wide on average, exhibits a number of meanders south of Africa. After an abrupt turnabout the Agulhas Return Current is observed to flow northeastwards more or less parallel to the Agulhas Current until obscured by cloud bands south of Port Elizabeth. A narrow filament of much colder water lies directly to the west of the retroflection, spreading laterally north of the current.

A clear depiction of the subsurface nature of the retroflection is given in Fig. 1a from the results of the Agulhas Current Project (Bang 1970). The depth of the sigma-*t* 25.80 clearly shows a number of the characteristic features of the region. The intense slopes made visible by the crowding of the 80 to 180 m isobaths delineate the outer border of the Agulhas and Agulhas Return Current. Offshore of Port Elizabeth a solitary, large meander in the current has been iden-

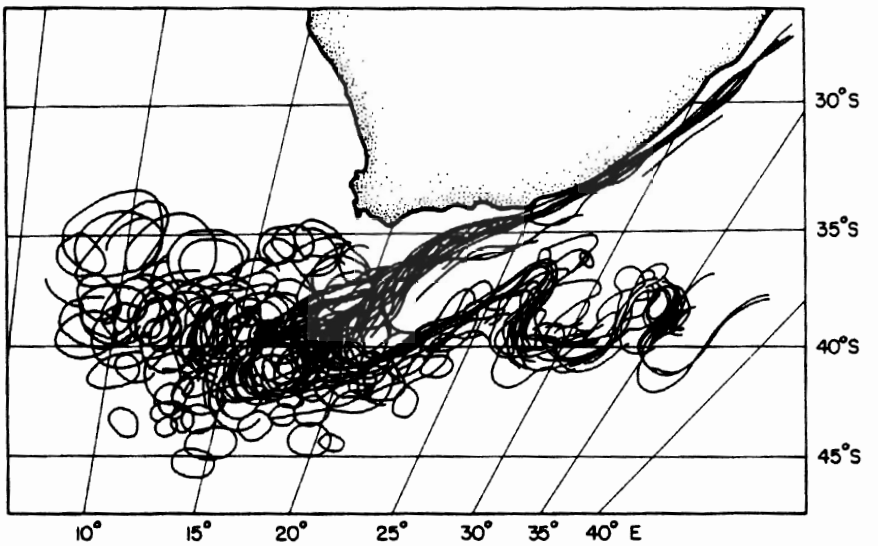

FIG. 2. Set of superimposed thermal borders of elements of the Agulhas Current for a period from December 1984 to December 1985. Images are declouded ones for the thermal infrared from METEOSAT II and only the most distinct one for every 12-day period was used.

TABLE 1. Locations and dimensions of Agulhas retroflection features from satellite infra-red sensing.

	1978	1979	1982	1983	All years
Total number of image days	337	361	318	95	1 111
Number of cloudpoor days	47	53	44	31	175
Cloud poor days as percentage	14%	15%	14%	33%	16%
Retroflection position for each event (B, Fig. 3)	17°26′	18°25′	18°36′	18°27′	18°15′°E
Maximum easterly retroflection position (B, Fig. 3)	19°45′	20°50′	25°30′	20°40′	20°30′°E
Maximum westerly position of warm features	9°40′	10°00′	12°00′	10°00′	9°40′°E
Mean diameters of retroflection loop (AC, Fig. 3) (km)	374	310	332	370	342
Standard deviation of loop diameter (km)	54	78	71	53	66

tified as a Natal Pulse (Lutjeharms and Roberts 1988). Downstream of this feature the current follows the continental shelf (not shown in Fig. 1a) quite closely, swinging abruptly south on passing the southernmost tip of the continental shelf at 20°E. On having completed the retroflection, the path of the Agulhas Return Current parallels that of the Agulhas Current proper. Two other important features are evident. The first is a very sharp meander in the Agulhas Return Current at about 27°E. It has been identified as a cold core eddy being spawned at the subtropical convergence (Lutjeharms and Valentine 1988). The second is a large eddy southwest of Cape Town, centered at 15°E. Between this eddy and Cape Town a significant meridional flux of predominantly Agulhas Current water is evident, similar to that established by Gordon (1985).

This general description of the circulation configuration at the Agulhas retroflection is supported by few direct current measurements to date. Buoys drifting down the Agulhas Current (Gründlingh 1978; Gründlingh and Lutjeharms 1979) passed through the retroflection with speeds of more than 100 cm s^{-1}, following the general portrayal of Fig. 1. Olson and Evans (1986) have reported speeds of between 20 and 80 cm s^{-1} around Agulhas rings, depending on the radial distance from the center of the ring.

Certain parts of the Agulhas system show some geographic permanence (Gründlingh 1983), while others show marked variability. Rapidly changing configuration is particularly evident when the positions of all the circulation features are superimposed (Fig. 2) for a full year. The intense thermal borders were used here to demarcate the location of the features. Crowding of lines indicates that up to 20°E the location of the Agulhas Current adjacent to the African continental shelf is very persistent. The most consistent easterly position of the retroflection can be identified as 20°E. An analysis of drifters which have passed through the area (Patterson 1985) shows that the highest surface speeds are also found here. Meridional meanders in the Agulhas Return Current lie predominantly at 27° and 32°E locations which agree with the conclusions reached by Lutjeharms and van Ballegooyen (1984) and Gründlingh (1978). A secondary location of the retroflection seems to lie at 16°E (Fig. 2). The westernmost extent of the retroflection is unclear, obscured as it is by a range of rings and/or eddies radiating from the retroflection. Warm circular features are observed westward to nearly 5°E, northward to 32°S and southward to 46°S. High rates of surface cooling (Lutjeharms and Gordon 1987; Walker and Mey 1987) of the newly spawned features may rapidly destroy their surface expressions. It is estimated that surface expressions may

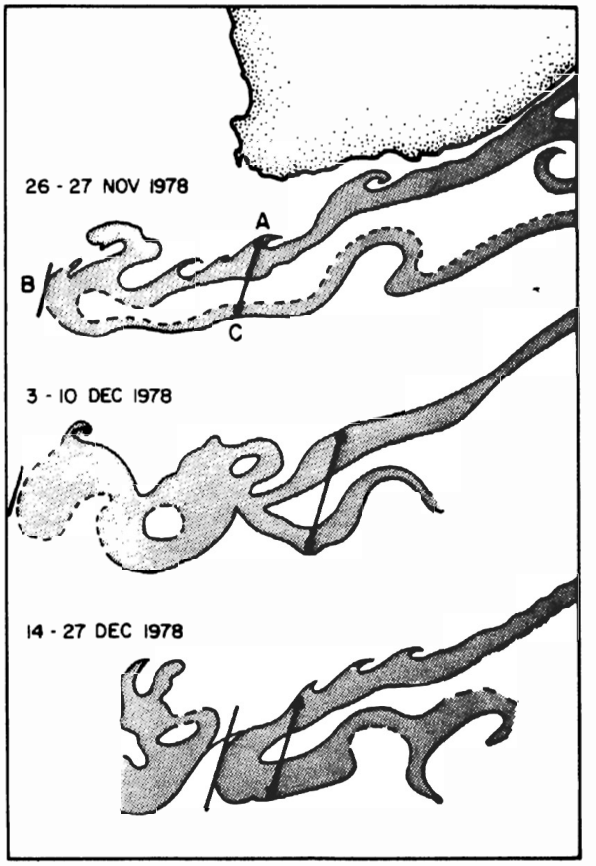

FIG. 3. The typical westward progradation (26–27 Nov), current coalescence (3–10 Dec) and ring-shedding behavior (14–24 Dec) of the Agulhas retroflection in 1978 (after Lutjeharms 1981b). Lettered positions show the locations where dimensions of the circulation were measured for this investigation: AC denotes the diameter of the retroflection loop; B the furthermost westward penetration of an intact retroflection loop. Infrared imagery is from METEOSAT I. An XBT section across this particular ring is presented in Fig. 12.

decay within a two-month period. Persistent cloudiness south of 45°S will also obscure much of the formation events and subsequent drift of eddylike features south of the retroflection. It may, therefore, be assumed that the area bordered by 32° to 46°S and 5° to 20°E is not the full range of influence of features shed from the Agulhas retroflection. Even so, this portrayal noticeably extends the possible geographic influence of the retroflection beyond those inferred by Harris et al. (1978), Gründlingh and Lutjeharms (1979), Bang (1970), Lutjeharms (1981a,b) or Sarukhanyan (1982).

The average location of features at the retroflection are given in Table 1 based on infrared data from the METEOSAT satellite series. The way in which the location of features and their dimensions have been defined for this purpose is depicted in Fig. 3. "Cloud poor" days have been defined as days for which cloud cover was sufficiently broken to allow unambiguous determination of mesoscale sea surface features. Each "event" consisted of a westward progradation and coalescence, and the mean longitudinal position for each event was calculated. Positions for the maximum east-

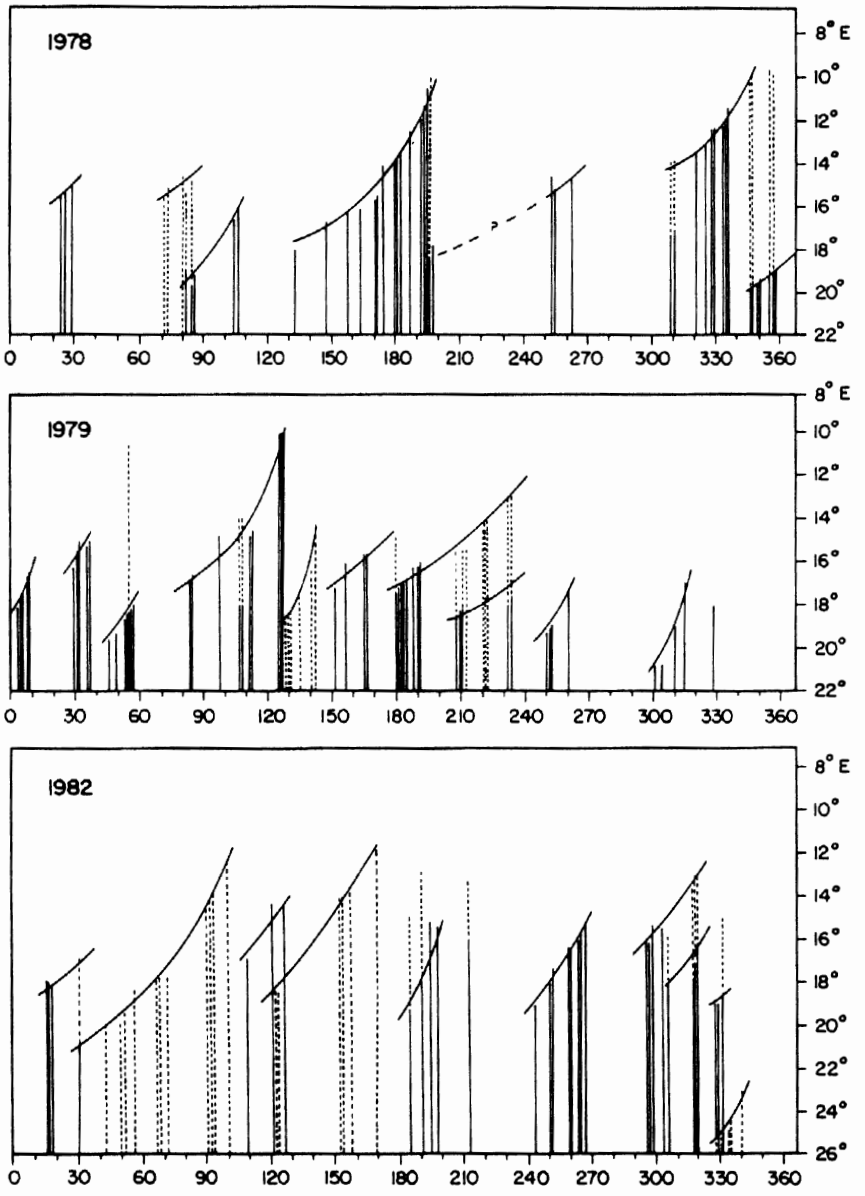

FIG. 4. Zonal location of the westernmost limit of the Agulhas Current retroflection for three full years from METEOSAT thermal infrared imagery. Abscissas are in year days. Solid lines denote an intact retroflection loop. Where rings had become detached or where cloudiness made it difficult to establish the unbroken nature of the retroflection loop, represented by dotted lines.

erly retroflection position, 20°30'E, agrees with the visual impression of this location from Fig. 2. The mean position of 18°15'E also seems consistent with that of Fig. 2, but the maximum westerly positions found in 1984–85 (Fig. 2) from declouded images were even further west than those for the four years of normal images for which statistics were obtained. The average diameter for the retroflection loop does not vary dramatically from year to year. The diameter established for 1978–79 (Lutjeharms 1981a) was 341 ± 72 km, while that for the four years given here was 342 ± 66 km.

4. Behavior of the Agulhas retroflection

The westward protrusion of warm Agulhas Current water (Fig. 3) may extend far into the South Atlantic. On thermal infrared imagery it is not always possible to distinguish between intact retroflection loops and contiguous series of Agulhas rings in satellite infrared images of this nature. Even without the ability to make this distinction, the occasional existence of broad zones of warm Agulhas water adjacent to the subtropical convergence in the southeast Atlantic Ocean and stretching over distances of over 500 km has not been recognized before and has important climatic and dynamic implications.

An analysis of penetrations of the Agulhas retroflection into the South Atlantic Ocean over a period of three years shows a number of consistent characteristics in the progradation behavior of the retroflection. A pictorial representation of these is given in Fig. 4. Each line in this figure represents one observation of the retroflection loop and vicinity on a sufficiently cloud poor day to facilitate detailed identification. It is immediately evident that observations are at irregular intervals with periods of a few to even as much as 50 days elapsing between good observations. The most noticeable characteristic of the progradations is that they occur as identifiable events. Within each event, westward penetrations show an increasing rate of progress with time followed by a sudden, discontinuous eastward jump. In all cases where sufficient imagery was available, this jump can be related directly to the shedding of an Agulhas ring (Fig. 3). In some cases the subsequent westward penetration of such a ring could also be followed. Progression rates of rings were observed to be similar to these of the Agulhas retroflection itself.

In cases where sufficient data were available (e.g., day 130 to 200, 1978, Fig. 4) the increase in rate of westward penetration with time was clearly evident. For those events where fewer data were available, it was not as clear. In some such cases the exact duration of events had to be surmised. To interpolate intermittent measurements a linear regression fit was carried out on each identified event. The mean rate of westward propagation is 12 cm s^{-1} while the mean duration of each event is 39 days (Table 2). A seasonal pattern is evident in neither. In many cases a slight degree of southerly penetration of the Agulhas retroflection loop was observed.

If the hypothesis that each progradation event culminates with the shedding of an Agulhas ring, the results from these three years (Fig. 4) suggest that on an average, nine rings are shed per year at intervals of slightly longer than a month. Olson and Evans (1986) have estimated that even two rings per year can replace the eddy energy calculated for the South Atlantic Ocean outside the direct influence of the Agulhas Current. Therefore, the shedding of nine rings per year, even if not all of them were to drift northwards, has significant implications for the energy contribution of these features to the total kinetic energy balance of the South Atlantic Ocean.

A detailed study of this ring-spawning process, as evident in satellite infrared imagery, shows that in almost all cases the shedding of a ring is preceded by the genesis and growth of a cold wedge of Sub-Antarctic Surface Water at the subtropical convergence. A sequence over a period of three weeks showing this phenomenon is portrayed in Fig. 5. Here, and in other schematic drawings (e.g., Figs. 6, 7 and 11), current directions were inferred from previous experience of analogous situations using drifters, hydrographic measurements and series of satellite imagery. From the onset of such a sharp angled disturbance on the convergence (on about 8 December) to its complete penetration through the retroflection loop, effectively separating newly created ring and mother current, took five days. Subsequently the most northerly extremity of this cold water mass spread laterally and mushroomed outward to cover a substantial area (see lowest panel, Fig. 5 as well as Fig. 1b).

Sea surface temperature difference between subantarctic water and South Atlantic surface water lends sufficient contrast to the northern border of this cold wedge; once this separation has been accomplished its lateral spreading can be followed. Sea surface temperatures obtained during the Agulhas Current Project (Bang 1970), in what might possibly have been such a feature, are below 18°C in March. Duncan (1968) found temperatures as low as 10°C which are clearly Sub-Antarctic by nature, as Lutjeharms and Valentine (1984) have shown that the mean temperature of the

TABLE 2. Statistics of prograding events of Agulhas retroflection.

	1978	1979	1982	1983	All years
Number of cloud poor days	47	53	44	31	175
Mean period of each event (days)	55	37	32	30	39
Mean rate of westward progradation (cm s^{-1})	7	13	14	15	12

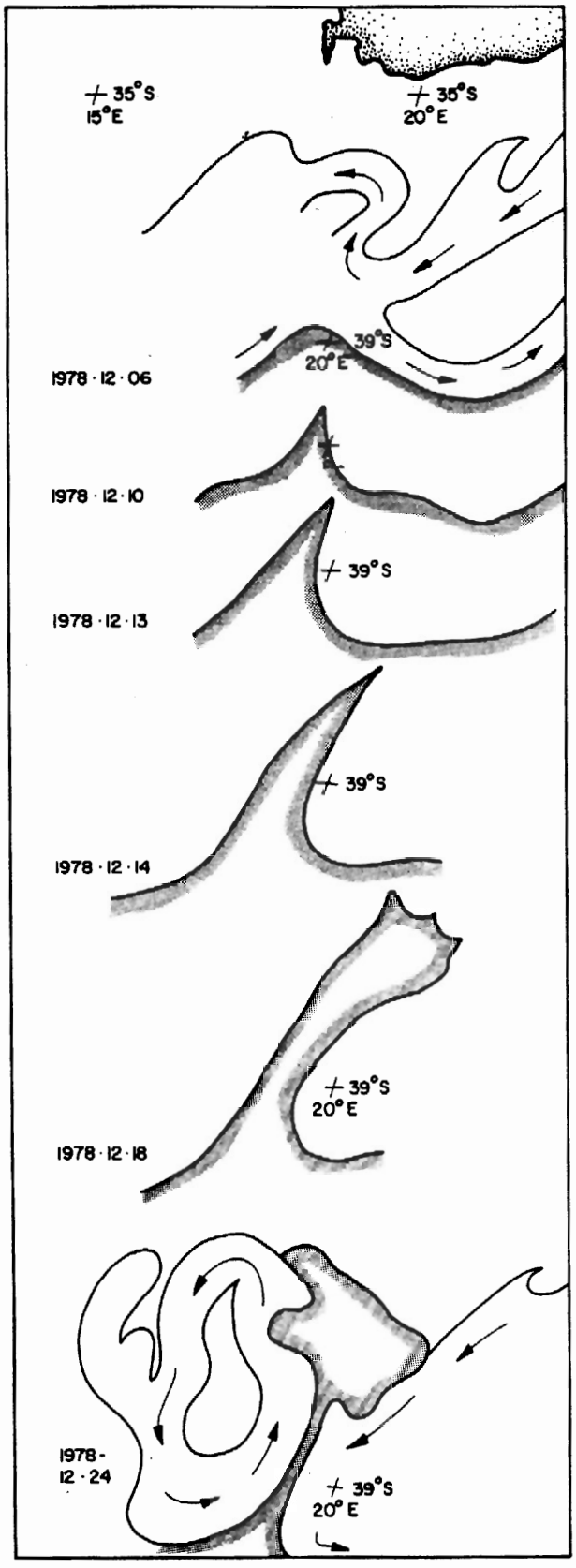

core of the subtropical convergence is 14°C. The average longitude of the cold wedge feature is 18°25′E (standard deviation 1°15′) and during the period of this investigation has been observed to penetrate to 36°15′S; in an extreme case even as far north as 35°S.

A sharp lateral wedge of water as described here implies opposing and nearly parallel currents for its maintenance. A series of conceptual images portraying the kinematics of such an event are set out in Fig. 6. Once the internal circulation within the loop has effectively been separated by such a meander (2) the opposing currents will establish a wedge-shaped border (3) which eventually penetrates equatorward separating the ring from the current (4). Note that this process in all observed instances proceeds from south to north and never the other way around.

The cold wedge conceivably may also be due to upwelling of colder water from greater depths. Historical temperature measurements previously mentioned would suggest that this upwelling would have to be from depths greater than about 300 m, which seems unlikely. Advection from south of the subtropical convergence remains a more promising supposition for the present. It is interesting to note that Boudra and de Ruijter (1986), using a wind-driven, baroclinic model, also show that Agulhas ring formation is due to a closing of the retroflecting current onto itself and, in particular, that interaction with the cold, low potential vorticity, eastward currents south of the retroflection area is also required for ring formation.

The spawning of rings in the manner described here may be influenced or precipitated directly by perturbations in the Agulhas Current itself. Lutjeharms and van Ballegooyen (1984) have shown that increases in the volume transport of the current may precipitate early retroflection, while it has also been suggested that the downstream growth of meanders may be agents of ring shedding (Lutjeharms 1981b). Gründlingh (1980) has demonstrated that small changes in the volume flux of the Agulhas Current occur but evidence for seasonal cycles is weak. Pearce and Gründlingh (1982) have in fact shown that no seasonal cycle is evident in the current core velocities of the current. The fact that the longitudinal position of the ring shedding is so well localized (Table 1, Fig. 2) suggests that the factors causing ring formation are reasonably well-behaved and not intermittent.

Modeling studies (Boudra and Chassignet 1988; Chassignet and Boudra 1988) indicate that factors influencing the frequency of ring shedding are dependent

FIG. 5. The characteristically rapid development and penetration of a cold wedge of Subantarctic Surface Water forming an inherent part of the spawning and separation of an Agulhas ring over a period of less than three weeks in December 1978. Thermal data were from METEOSAT I. A section through this ring is shown in Fig. 7.

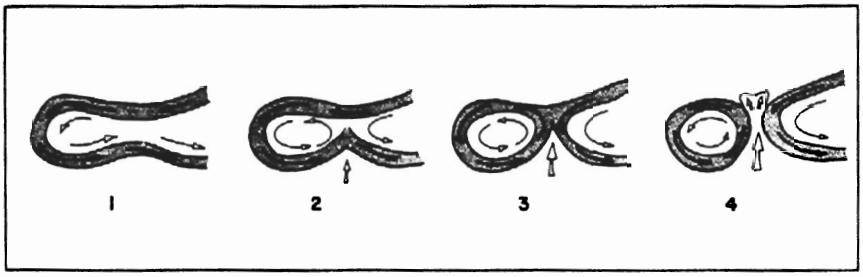

FIG. 6. Conceptual image of the initiation (2), development (3) and separation (4) of an Agulhas ring from the Agulhas retroflection.

on the southward inertia of the Agulhas Current and on the degree of slippage between the current and the African continent. In high Rossby number experiments, rings appear to develop owing to instability in the Return Current.

5. Associated features of the Agulhas retroflection

A number of ring and eddylike features have been observed to be associated with the Agulhas retroflection (Fig. 2). Rings are here considered to be that subset of eddies which exhibit very definitive annulus characteristics. Three features in particular are singled out for further description; namely, the rings to the west of the retroflection as identified, eddies to the south of the subtropical convergence and rings no longer noticeable by their distinctive thermal expression at the sea surface.

An example of a well-defined, recently spawned Agulhas ring to the west of the retroflection is portrayed in Fig. 7. Clearly evident is the retroflection loop characteristically lying at 20°E directly after spawning of a

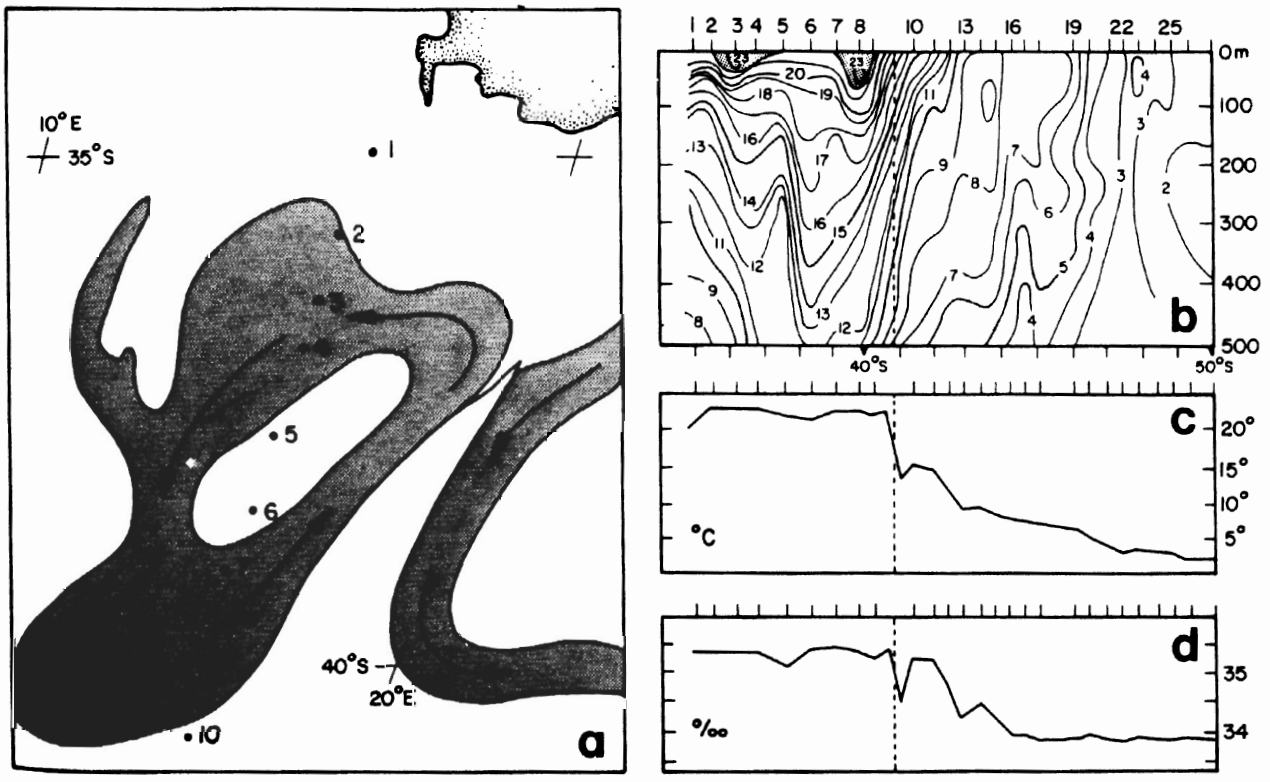

FIG. 7. The disposition and vertical dimensions of an Agulhas ring in December 1978. The portrayal of the surface features (a) is according to infrared data from METEOSAT I for the period 13 to 24 December 1978 (see also Fig. 5 for spawning sequence). The vertical temperature section (b) is from XBTs launched at the station positions bisecting the ring (a). That part of the water column warmer than 22°C has been shaded in (b), while the dashed line shows the core of the subtropical convergence. Concurrent measurements of surface temperatures (c) and surface salinities (d) are presented. Solid arrows denote inferred flow directions.

ring. A distinctive wedge of cold Sub-Antarctic Water separates the ring from the retroflection loop. The ring has an elliptical configuration with evidence of some shear-edge features. The annulus-type water distribution in the surface layers is also evident from the thermal section shown in Fig. 7b. The southern part of the ring lies adjacent the subtropical convergence as determined from the surface temperature (c), surface salinity (d) and the subsurface temperatures (b). Surface temperatures and the thermal structure of the upper layers of the ring are identical to those found in the southern Agulhas Current during this time of year (Gordon 1985; Harris and van Foreest 1978). Using observations based on stations much more widely spaced, Duncan (1968) found a very similar configuration with a near-identical vertical depression of the 12°C isotherm from about 200 m to 600 m.

The geographic distribution of rings of this nature is intimated in Fig. 2. This distribution was for a full year. An example of the distribution on one, perhaps representative, occasion is portrayed in a thermal infrared image of 9 February 1985 (Fig. 8). Although partially obscured by clouds, a clear Agulhas retroflection loop stretches to 16°E. Between here and 13°E a near-circular Agulhas ring is evident, bordered on the eastward side by a cold wedge. To the west lies a ring with a fainter surface expression. At least eight other circular mesoscale features may be inferred from their distinctive surface temperature distributions or from encircling filaments of water with distinctively contrasting surface temperatures. Gordon et al. (1987) have shown the characteristics of two rings present simultaneously, while Olson and Evans (1986) have shown that these rings translated northwestwards at speeds of 4.8 to 8.5 cm s^{-1}. The distribution of rings indicated by Fig. 8 may therefore be quite a characteristic portrayal of the disposition of features spawned at the retroflection during a number of previous events and their subsequent translations, radiating outward from the retroflection source.

Rings or eddies to the south of the subtropical convergence are seldom identified in satellite imagery because of persistent cloud cover. Nevertheless, Lutjeharms and Valentine (1988) have assembled a sufficient collection of examples to distinguish between eddies created at the southern border of the retroflection, probably by shear or baroclinic instabilities, and true pinchings-off of Agulhas rings. Colton and Chase (1983) have followed a feature from satellite altimetry which from its location would seem a prime candidate for an Agulhas ring. It had a diameter of 250 km, circular velocities of 90–100 cm s^{-1} and moved southeastward at an average 7 cm s^{-1}. Lutjeharms (1988) has described the budding off of a warm eddy across the subtropical convergence and its subsequent drift in the Sub-Antarctic zone, while Sarukhanyan (1982) identified at least two intense and three less intense mesoscale eddylike features south of the convergence.

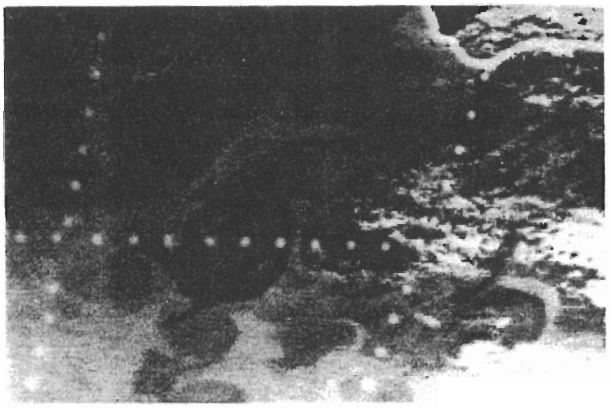

FIG. 8. An image from METEOSAT II for 9 February 1985 showing the location of more than nine identifiable Agulhas rings and eddies in the retroflection region of the Agulhas Current, south of the subtropical convergence and in the adjacent southeast Atlantic Ocean.

Therefore, it is clear that features spawned at the Agulhas retroflection may propagate south of the subtropical convergence although it is not clear what portion of these are true rings.

In Fig. 9a an interpretive line drawing of a satellite image of such a feature is shown. A narrow neck of warm surface water still connects the feature to its mother body of warm water, namely, the Agulhas retroflection. The line of XBT stations lay northwest of this neck and this shows the features of a distinctly separate warm eddy (Fig. 9b). Both its internal thermal structure, demonstrated by the depth of individual isotherms, the surface temperature (c), as well as the surface salinity (d), portray the eddy as having typical Agulhas Current core characteristics. The thermal section shows a diameter of 150 km, but the satellite image indicates an elliptical circumference (see also Fig. 7) so that the minor axis may be smaller. The average width of the current being about 90 km (Pearce 1977), a feature with a diameter less than 150 km would not be expected to contain a core of cooler loop water. This eddy, therefore, cannot be considered to be a true Agulhas ring.

Some satellite images of the area (Fig. 10) show warm water features with undifferentiated surface temperatures, i.e., discs with more or less the same surface temperature throughout, as well as distinct rings of warmer water with higher temperatures in an annulus shape, i.e., with slightly cooler water in the center. The infrared image for 4 December 1985 (Fig. 10a) shows a ring directly to the west of the retroflection loop, as well as a circular, well-defined ring to the southeast of the loop. Both exhibit diameters very similar to the retroflection loop, as well as (uncorrected) radiance values nearly identical to those found in the Agulhas Current core at the retroflection. The warm feature partially visible on 15 August 1985 (Fig. 10b) has slightly lower radiance values and would seem to

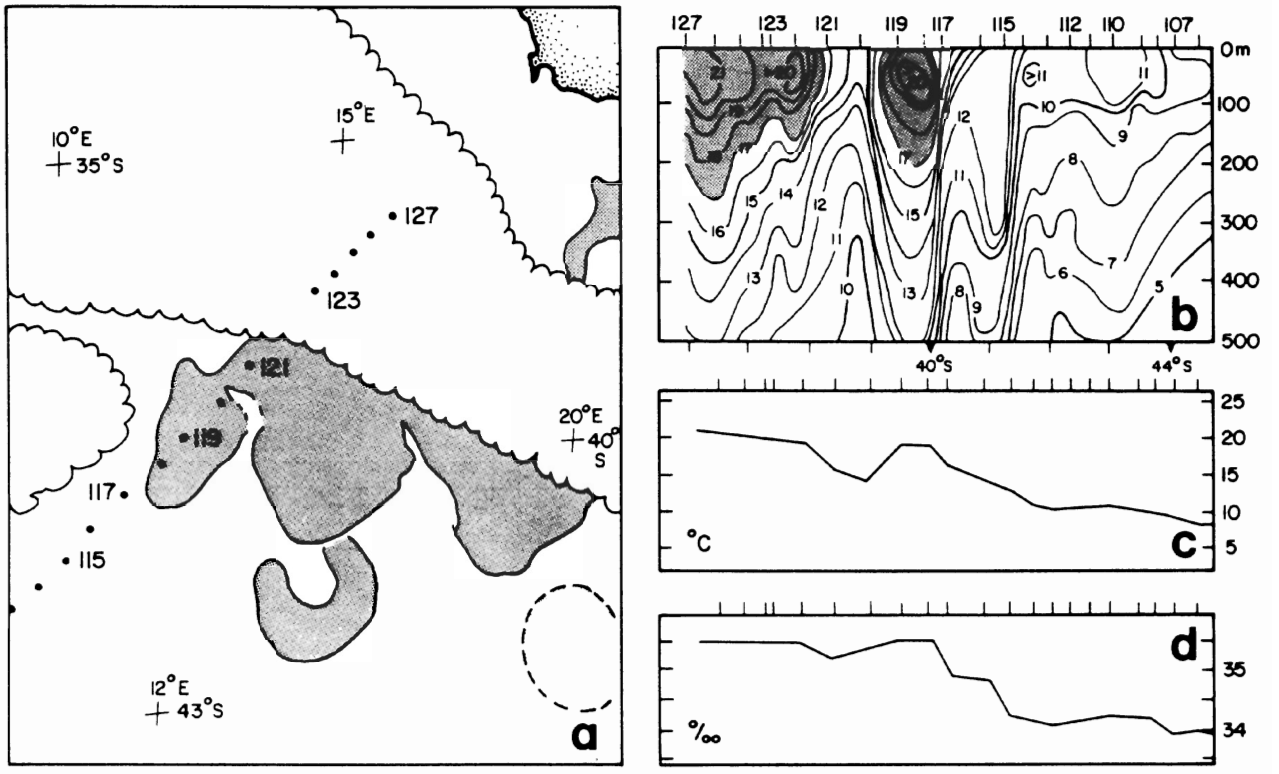

FIG. 9. (a) An interpretive line drawing of a warm eddy south of the subtropical convergence at the Agulhas retroflection according to a NIMBUS 7 CZCS thermal infrared image (No. 1966) for 15 March 1979. Station positions shown are for the XBT section from which the temperature section is shown in (b). Water warmer than 17°C has been shaded. Results of the concurrent measurements of sea surface temperature and salinity are shown in (c) and (d) respectively.

be slightly larger than the retroflection loop of that period. A range of features of this nature are visible in satellite imagery (e.g., see Fig. 8). Since it has been shown (Lutjeharms and Gordon 1988) that the warm surface water of an annulus will spread across the center of a ring, it is impossible to establish how many of these features are true rings by their surface expressions only.

Owing to the persistent cloudiness it is very unusual to obtain a sufficiently lengthy cloudpoor satellite image series to establish the propagation of warm features south of the subtropical convergence. The average drift velocities of drifting buoys in the area is eastward (Patterson 1985; Lutjeharms and Valentine 1987; Gründlingh and Lutjeharms 1979). In some recorded instances this does not seem to affect the warm features (Lutjeharms 1988) but in most observed cases features, whether rings or not, shed at the retroflection across the subtropical convergence, propagate eastwards. The general distribution of such features (Fig. 2) shows only three east of 20°E. Their distinctive surface expressions may, however, be lost to the atmosphere so rapidly (Walker and Mey 1988) that this distribution may be too confined. Lutjeharms and Valentine (1988) have reported a number of features further to the east based on XBT-sections, which seems to support the contention that rings are more prevalent here than indicated by sea surface temperatures.

The rapid cooling of the surface layers of Agulhas rings spawned at the Agulhas retroflection and drifting northward limits the reliability of ring distributions for this area as well. Lutjeharms and Gordon (1988) have described details of an Agulhas ring situated off Cape Town of which the surface characteristics showed no thermal contrast to their surroundings until filaments of warm Agulhas Current water, advected into the area, were drawn around the feature thus showing its location and dimensions. Similar effects of warm and cold filaments delineating subsurface features are evident in Fig. 8 and 11. Simpson et al. (1984) have reported similar inflows of coastal water into offshore eddies off California. This mechanism may constitute a significant flow of surface water from the Indian to the Atlantic Ocean. The rate of temperature change of the surface layers of rings may also be materially affected if atmospheric cooling is counteracted by continual influx of warm Agulhas water.

6. Discussion

Although exceptional in its complete retroflection, the ring shedding from the Agulhas Current is not un-

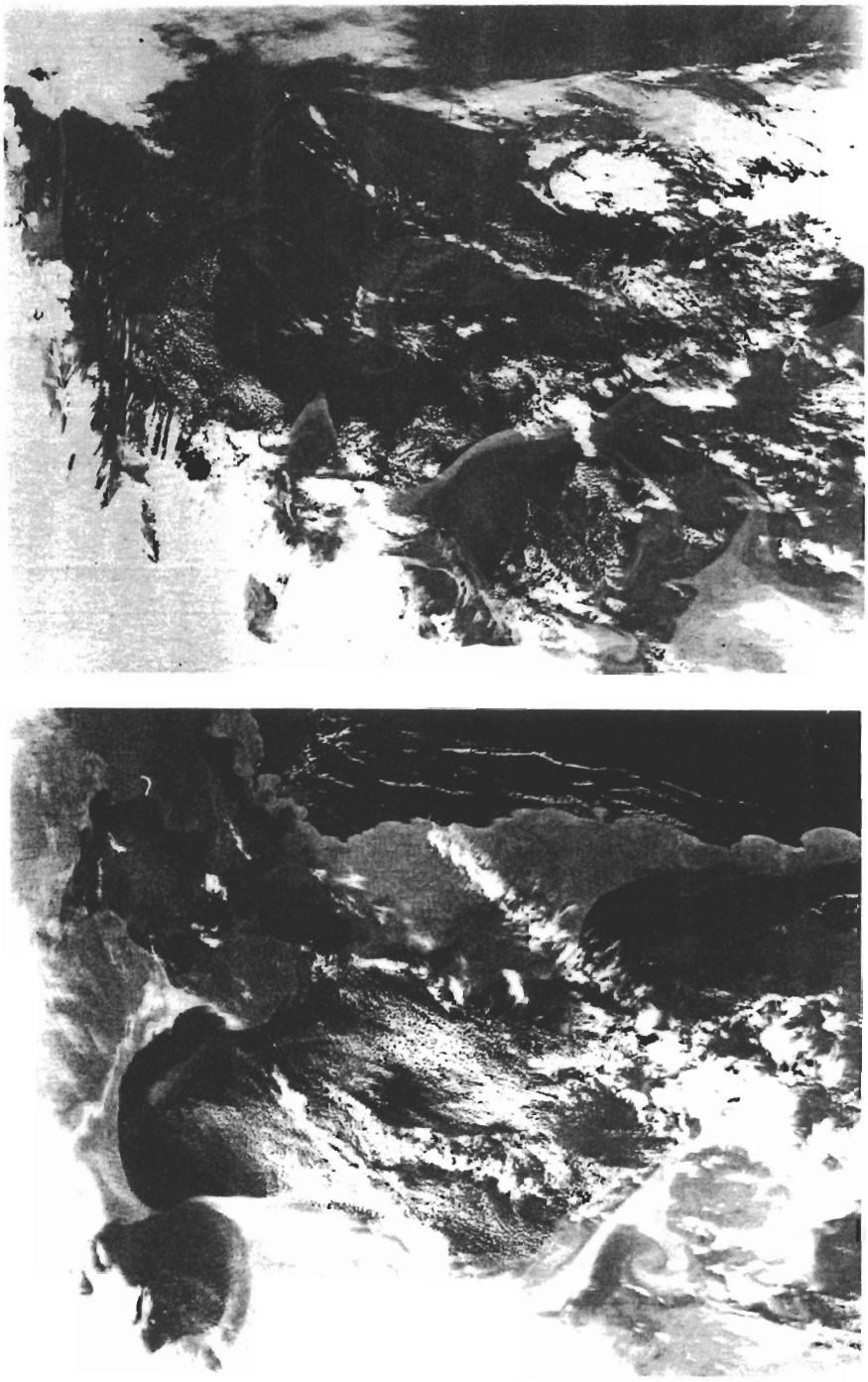

FIG. 10. Example of (a) an Agulhas ring well south of the subtropical convergence and the Agulhas retroflection. The thermal infrared image is from the NOAA 9 AVHRR for 4 December 1985; (b) an Agulhas ring recently shed to the south of the main retroflection (NOAA 9, 15 August 1985).

usual for a western boundary current because ring shedding from the Gulf Stream (Fuglister 1972), the Kuroshio (Solomon 1978), the East Australian Current (Nilsson and Cresswell 1981) and the Brazil Current (Legeckis and Gordon 1982) are either well known or have been recognized. Rates of shedding are very different. Whereas this analysis indicates an average of 9 ring sheddings per year for the Agulhas Current, Legeckis and Gordon (1982) claim one a week for the Brazil Current. The progradation events for this current

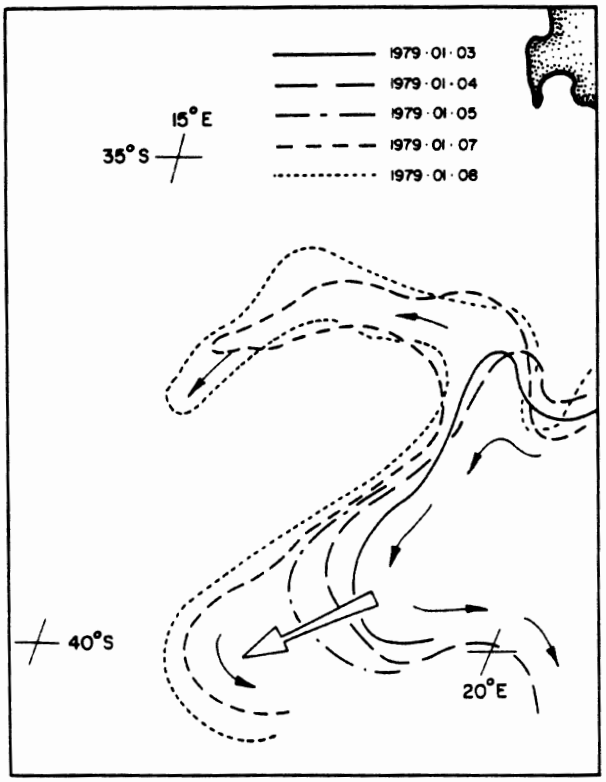

FIG. 11. Westward penetration of the Agulhas retroflection over a 5-day period (open arrow). Note also the anticyclonic advection of a warm filament of water lying further north. Solid arrows show the inferred flow directions.

occur at intervals of about two months which is in closer agreement with that of the Agulhas Current. According to Nilsson and Cresswell (1981) only two rings per year are formed at the East Australian Current. For currents which do carry out a semiretroflection, all in the Southern Hemisphere, the rate of ring shedding by the Agulhas Current seems high.

The upstream or downstream drift of rings and their subsequent reabsorption by the mother current has been observed in the Gulf Stream (The Ring Group 1981), the Kuroshio (Solomon 1978) and the East Australian Current (Nilsson and Cresswell 1981). The coalescence of cast-off rings has also been observed (Cresswell 1981). No events of this nature have as yet been observed for the Agulhas Current. Leakage of warm water from the East Australian Current to adjacent eddies (Nilsson and Cresswell 1981) is a feature which has also been observed for eddies cast off from the Agulhas Current south of the subtropical convergence (Lutjeharms 1988), eddies which may "scavenge" warm surface water from the Agulhas Return Current without being reabsorbed across the convergence.

No estimates have been made for the lifetime of Agulhas rings. McCartney et al. (1988) have described an anticyclonic eddy along the eastern side of the mid-Atlantic ridge at 5°W and 23°S. According to the translation rates calculated by Olson and Evans (1986), this would imply an age of 2.2 years, if this indeed were an Agulhas ring. Nilsson and Cresswell (1981) have estimated an average lifetime of 650 days for East Australian Current eddies, which compares favorably with that estimated for Gulf Stream Rings (Lai and Richardson 1977). The Ring Group (1981) estimate an even longer lifetime of up to four years, suggested by the decay rate. Agulhas rings can be expected to have similar durations.

The influence of Agulhas rings on the South Atlantic Ocean by the additional energy input may be substantial (Olson and Evans 1986). This influence and the meridional energy transfer is dependent on the trajectories of the rings and their subsequent geographic distribution. The distribution of Gulf Stream rings in the North Atlantic has been studied in some detail (Richardson 1980; Richardson et al. 1978) and has been shown to be extensive. The drift of eddies cast off from the East Australian Current (Nilsson and Cresswell 1981) as well as the Brazil Current (Legeckis and Gordon 1982) has, however, been shown to be small. In many cases the effect of mid-ocean or other ridges on the area in which rings or eddies are to be found is significant (Dantzler 1976; Roden et al. 1982; Bernstein

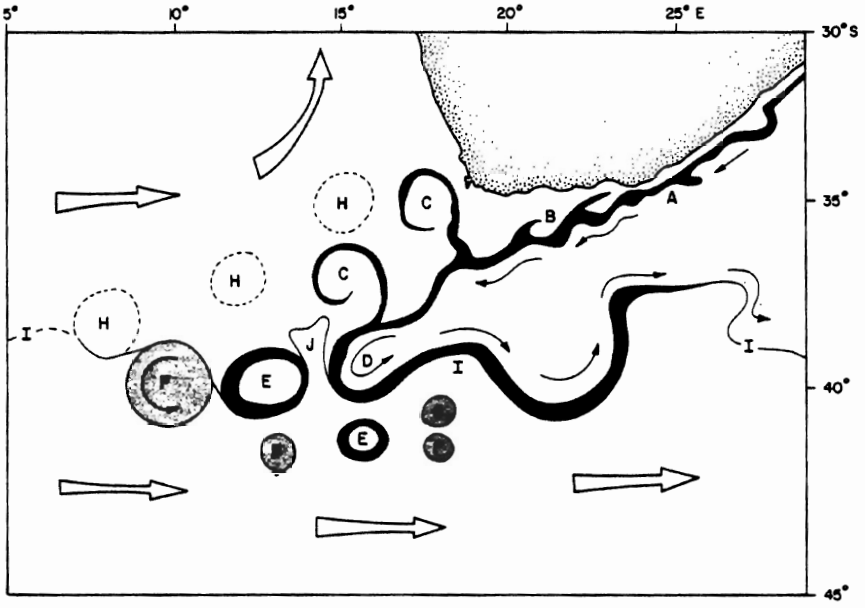

FIG. 12. A conceptual image, based on 7 years of satellite imagery and XBT sections, of the Agulhas retroflection and environment. Broad open arrows show mean drift patterns, while solid arrows show the current direction in the southern reaches of the Agulhas current. Lettered features are: A, the narrow, well-defined surface expression of the Agulhas Current adjacent the narrow continental shelf of southeastern Africa; B, meanders in the current path next to the Agulhas Bank; C, Agulhas rings delineated by warm Agulhas Current filaments; D, the Agulhas retroflection loop; E, newly spawned Agulhas rings of which surface features are still identifiably rings; F, older Agulhas rings which can no longer be unambiguously identified as rings by their surface expressions alone; G, a warm eddy south of the subtropical convergence, having been shed in the vicinity of the subtropical convergence; H, older Agulhas rings no longer evident by surface expressions; I, the subtropical convergence; J, wedge of cold Sub-Antarctic water.

and White 1981). The ring-shedding area of the Agulhas retroflection is bordered by the Atlantic–Indian midocean ridge to the south, the Atlantic midocean ridge to the west and the Walvis Ridge to the north. The implications of these ridges for the eddy or ring distribution are as yet unknown.

7. Conclusions

The conclusions of this descriptive investigation may best be summarized by reference to the conceptual image presented in Fig. 12.

1) The Agulhas retroflection lies between 20° and 16°E (Fig. 12; D). The mean diameter of the retroflection loop is 342 km and the most westerly position of warm surface water derived from the Agulhas Current is 9°40′E for the period under investigation.

2) The zonal location of the Agulhas retroflection is not stable but shows a characteristic progradation into the South Atlantic and sudden subsequent reinitiation in the east with average periods of 39 days for each event. The mean rate of westward progradation is 12 cm s^{-1} and on an average, nine events per year.

3) Each progradation event is concluded with the shedding of a warm-core Agulhas ring with an average diameter of 307 km (Fig. 12; F, E). The shedding of most rings is preceded by the genesis and growth of a telltale wedge of cold Sub-Antarctic Surface Water (Fig. 12; J) proceeding from the south and separating the newly-formed ring from the Agulhas retroflection loop now lying much further east.

4) Rings shed at the Agulhas retroflection may move westwards, rapidly losing their distinct surface thermal expression (Fig. 12; E, F, H); southward where, in addition, persistent cloudiness will obscure them (Fig. 12; E, F, G) or northward where occasional filaments of warm Agulhas Current water may delineate them, particularly off Cape Town (Fig. 12; C). It is assumed, therefore, that this whole ocean area is populated by a range of rings and eddies in various stages of decay. Those that have been observed by hydrographic measurements extend to the full depth of the measurements made in each case. Little is known about rates of translation.

5) The behavior of the Agulhas retroflection and the shedding of rings is analogous to similar features of other western boundary currents of the Southern Hemisphere, but more intense. In contrast to other western boundary currents no reabsorption events or eddy-coalescence events have as yet been observed. Lifetimes exceeding two years have been suggested for Agulhas rings.

Acknowledgments. We thank the personnel of the Satellite Remote Sensing Centre of the South African CSIR at Hartebeeshoek and of the NESS/NOAA in the United States for invaluable help in obtaining suitable satellite imagery. Measurements at sea were made by a large number of colleagues and volunteers who are mentioned by name elsewhere. The typing of the manuscript was done by Mrs. M. Els, while Mrs. B. Theron did the draughting. This research was supported by the Antarctic Programme of the South African Scientific Committee for Antarctic Research (SASCAR) and by the South African National Committee for Oceanic Research (SANCOR).

REFERENCES

Bang, N. D., 1970: Dynamic interpretations of a detailed surface temperature chart of the Agulhas Current retroflexion and fragmentation area. *S. Afr. Geogr. J.*, **52**, 67–76.

Bernstein, R. L., and W. B. White, 1981: Stationary and travelling mesoscale perturbations in the Kuroshio Extension Current. *J. Phys. Oceanogr.*, **11**, 692–704.

Boudra, D. B., and W. P. M. de Ruijter, 1986: The wind-driven circulation in the South Atlantic–Indian Ocean—II. Experiments using a multi-layer numerical model. *Deep-Sea Res.*, **33**, 447–482.

——, and E. P. Chassignet, 1988: Dynamics of Agulhas retroflection and ring formation in a numerical model. I. The vorticity balance. *J. Phys. Oceanogr.*, **18**, 280–303.

Boyle, T. P., and S. R. Howe, 1985: Dealing with digital data from current meteorological and earth resources satellites. *Proc., EDIS 83, Earth Data Information Systems Symp.*, Pretoria, South Africa, 17 pp.

Chassignet, E. P., and D. B. Boudra, 1988: Dynamics of Agulhas retroflection and ring formation in a numerical model. II. Energetics and ring formation. *J. Phys. Oceanogr.*, **18**, 304–319.

Colton, M. T., and R. R. P. Chase, 1983: Interaction of the Antarctic Circumpolar Current with bottom topography: An investigation using satellite altimetry. *J. Geophys. Res.*, **88**, 1825–1843.

Cresswell, G. R., 1981: The coalescence of two East Australian Current warm-core eddies. *Science*, **215**, 161–164.

Dantzler, H. L., 1976: Geographic variations in intensity of the North Atlantic and North Pacific oceanic eddy fields. *Deep-Sea Res.*, **23**, 783–794.

de Ruijter, W. P. M., 1982: Asymptotic analysis of the Agulhas and Brazil Current systems. *J. Phys. Oceanogr.*, **12**, 361–373.

——, and D. B. Boudra, 1985: The wind-driven circulation in the South Atlantic–Indian Ocean—I. Numerical experiments in a one-layer model. *Deep-Sea Res.*, **32**, 557–574.

Duncan, C. P., 1968: An eddy in the subtropical convergence southwest of South Africa. *J. Geophys. Res.*, **73**, 531–534.

Fuglister, F. C., 1972: Cyclonic Gulf Stream rings formed by the Gulf Stream 1965–66. *Studies in Physical Oceanography, Vol. 1*, Gordon and Breach, 137–167.

Gill, A. E., and E. H. Schumann, 1979: Topographically induced changes in the structure of an inertial coastal jet: Application to the Agulhas Current. *J. Phys. Oceanogr.*, **9**, 975–991.

Gordon, A. L., 1985: Indian–Atlantic transfer of thermocline water at the Agulhas Retroflection. *Science*, **227**, 1030–1033.

——, J. R. E. Lutjeharms and M. L. Gründlingh, 1987: Stratification and circulation at the Agulhas Retroflection. *Deep-Sea Res.*, **34**, 565–599.

Gründlingh, M. L., 1978: Drift of a satellite-tracked buoy in the southern Agulhas Current and Agulhas Return Current. *Deep-Sea Res.*, **25**, 1209–1224.

——, 1980: On the volume transport of the Agulhas Current. *Deep-Sea Res.*, **27**, 557–563.

——, 1983: On the course of the Agulhas Current. *S. Afr. Geogr. J.*, **65**, 49–57.

——, and J. R. E. Lutjeharms, 1979: Large-scale flow patterns of the Agulhas current system. *S. Afr. J. Sci.*, **75**, 269–270.

Harris, T. F. W., and D. van Foreest, 1978: The Agulhas Current in March 1969. *Deep-Sea Res.*, **25**, 549–561.

——, R. Legeckis and D. van Forest (sic), 1978: Satellite infrared images in the Agulhas Current system. *Deep-Sea Res.*, **25**, 543–548.

Lai, D. Y., and P. L. Richardson, 1977: Distribution and movement of Gulf Stream rings. *J. Phys. Oceanogr.*, **7**, 670–683.

Legeckis, R., and A. L. Gordon, 1982: Satellite observations of the Brazil and Falkland Current. *Deep-Sea Res.*, **29**, 375–401.

Lutjeharms, J. R. E., 1981a: Spatial scales and intensities of circulation in the ocean areas adjacent to South Africa. *Deep-Sea Res.*, **28**, 1289–1302.

——, 1981b: Features of the southern Agulhas Current circulation from satellite remote sensing. *S. Afr. J. Sci.*, **77**, 231–236.

——, 1988: Meridional heat transport across the subtropical convergence by a warm eddy. *Nature*, **331**, 251–253.

——, and W. J. Emery, 1983: The detailed thermal structure of the upper ocean layers between Cape Town and Antarctica during the period Jan–Feb 1978. *S. Afr. J. Antarc. Res.*, **13**, 3–14.

——, and R. C. van Ballegooyen, 1984: Topographic control in the Agulhas Current system. *Deep-Sea Res.*, **31**, 1321–1337.

——, and H. R. Valentine, 1984: Southern Ocean thermal fronts south of Africa. *Deep-Sea Res.*, **31**, 1461–1476.

——, and H. R. Roberts, 1988: The Natal Pulse; an extreme transient on the Agulhas Current. *J. Geophys. Res.*, **93**, 631–645.

——, and H. R. Valentine, 1988: The formation of eddies at the subtropical convergence south of Africa. *J. Phys. Oceanogr.*, in press.

——, and A. L. Gordon, 1987: Shedding of an Agulhas Ring observed at sea. *Nature*, **325**, 138–140.

——, and A. L. Gordon, 1988: Kinematical behaviour of the surface layers at the Agulhas retroflection over a three month period. *Deep-Sea Res.*, in preparation.

McCartney, M. S., M. E. Raymer and C. A. Collins, 1988: A deep reaching anticyclonic eddy in the subtropical gyre of the eastern South Atlantic. In preparation.

Nilsson, C. S., and G. R. Cresswell, 1981: The formation and evolution of East Australian Current warm-core eddies. *Progress in Oceanography*, Vol. 9, Pergamon, 133–183.

Olson, D. B., and R. H. Evans, 1986: Rings of the Agulhas. *Deep-Sea Res.*, **33**, 27–42.

Patterson, S. L., 1985: Surface circulation and kinetic energy distributions in the Southern Hemisphere oceans from FGGE drifting buoys. *J. Phys. Oceanogr.*, **15**, 865–884.

Pearce, A. F., 1977: Some features of the upper 500 m of the Agulhas Current. *J. Mar. Res.*, **35**, 731–751.

——, and M. L. Gründlingh, 1982: Is there a seasonal variation in the Agulhas Current? *J. Mar. Res.*, **40**, 177–184.

Richardson, P. L., 1980: Gulf Stream ring trajectories. *J. Phys. Oceanogr.*, **10**, 90–104.

——, R. E. Cheney and L. V. Worthington, 1978: A census of Gulf Stream rings. *J. Geophys. Res.*, **83**, 6136–6144.

The Ring Group, 1981: Gulf Stream cold-core rings: Their physics, chemistry, and biology. *Science*, **212**, 1091–1100.

Roden, G. I., B. A. Taft and C. C. Ebbesmeyer, 1982: Oceanographic aspects of the Emperor seamounts region. *J. Geophys. Res.*, **87**, 9537–9552.

Sarukhanyan, E. I., 1982: The three-dimensional structure of the west wind drift in the region between Africa and Antarctica. *Dokl. Akad. nauk SSSR*, **250**, 234–237.

Simpson, J. J., C. J. Koblinsky, L. R. Haury and T. D. Dicky, 1984: An offshore eddy in the California Current system. *Progress in Oceanography*, Vol. 13, Pergamon, 1–111.

Solomon, H., 1978: Detachment and recombination of a current ring with the Kuroshio. *Nature*, **274**, 580–581.

Walker, N. D., and R. D. Mey, 1988: Ocean/atmosphere heat fluxes within the Agulhas Retroflection region. *J. Geophys. Res.*, in press.